Chapter 2
Measurements of ECTO-NOX (ENOX) Activities

A major challenge in ENOX discovery and validation has been limitations imposed by methods of measurement of ENOX activities. Thus far, measurement opportunities for the oxidative activity have been restricted to NAD(P)H, the natural electron donors (hydroquinones such as coenzyme Q in animals (Kishi et al. 1999) and vitamin K_1 hydroquinone in plants (Bridge et al. 2000)) and electron acceptors for the oxidative activities of molecular oxygen (Morré et al. 1998a; Orczyk et al. 2005) and protein disulfides (Chueh et al. 1997a) and substrates that support protein disulfide-thiol interchange. Except for certain tetrazolium dyes and despite exhaustive studies, artificial dye donors and/or acceptors, frequently utilized with NADH dehydrogenases, have not been discovered for ENOX proteins. Measurements of protein disulfide-thiol interchange activity have utilized primarily activation of inactive ribonuclease A and cleavage of dithiodipyridine (DTDP) derivatives (Sects. 2.6, 2.7, and 2.8). Protein may be estimated by the method of Smith et al. (1985) with bovine serum albumin as the standard.

Despite their widespread use as ENOX substrates, NADH or NADPH are artificial donors. Their use has been predicated principally on convenience and the historical precedent of ENOX discovery based on NADH oxidation (Morré 1998c). Specific activities are low, in the 10–20 μmol/min/mg of recombinant protein purified to homogeneity giving rise to very small turnover numbers (the number of substrate molecules converted to product per minute with the enzyme fully saturated with substrate) of 200–500 for NADH oxidation (Table 1.4). Rates of oxidation of natural hydroquinone or other substrates contained within the plasma membrane or in biological fluids most often require measurement in the nmol/min/mg protein range. Yet in well-synchronized ENOX preparations, NADH oxidation rates oscillate between rapid and slow to create reproducible and statistically significant recurring patterns within each period. In this chapter, spectroscopic approaches to rate analyses are described that validate the basic oscillatory phenomenon associated with ENOX proteins. Our approaches to the measurement of low rates of NADH oxidation are based on least squares slopes of spectrophotometric traces along with statistical evaluations of the reproducibility of the oscillatory patterns.

D.J. Morré and D.M. Morré, *ECTO-NOX Proteins: Growth, Cancer, and Aging*,
DOI 10.1007/978-1-4614-3958-5_2, © Springer Science+Business Media New York 2013

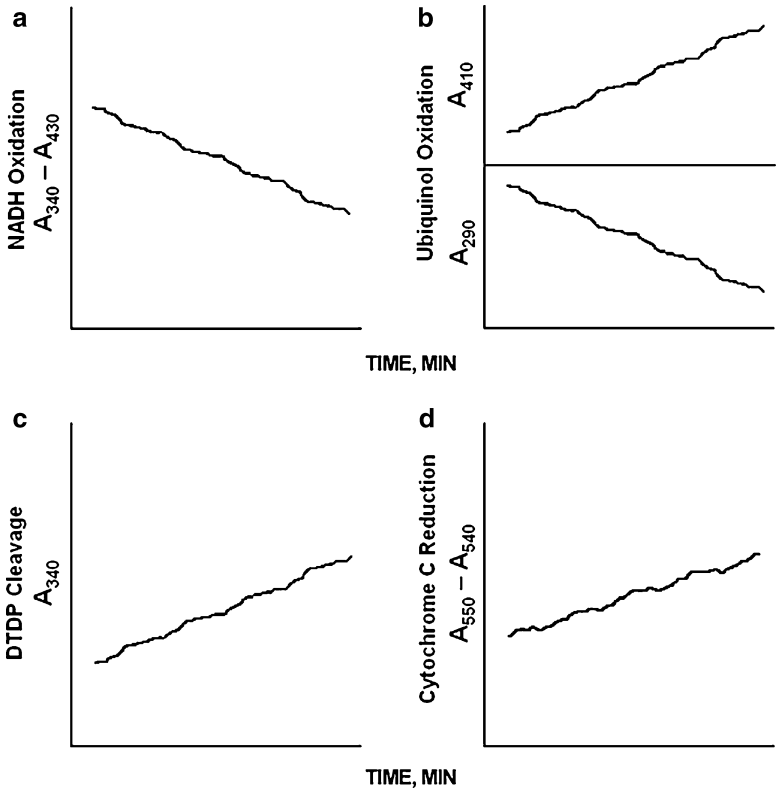

Fig. 2.1 Schematic representation of primary spectrophotometric assays used in the characterization of oscillatory activities. (**a**) The standard NADH oxidase activity that records the decrease in A_{340} resulting from NADH oxidation with reference at A_{430}. (**b**) Hydroquinone oxidation indicated by increasing absorbance at A_{410} or decreasing absorbance at A_{290}. (**c**) Cleavage of dithiodipyridine (DTDP) resulting in increased absorbance at A_{340} as a measure of protein disulfide-thiol interchange. (**d**) Reduction of cytochrome c (increase in A_{550} with reference at A_{540}) used as a measure of superoxide production by arNOX proteins (Chap. 9)

The four principal spectrophotometric assays to monitor periodicity of ENOX activities are illustrated diagrammatically in Fig. 2.1. The standard NOX assay (Fig. 2.1a) measures NADH oxidation (Sect. 2.1). The quinone oxidation assay (Fig. 2.1b) measures either an increase in absorbance of A_{290} or a decrease in absorbance at A_{410} (Sects. 2.4.1 and 2.4.2). Protein disulfide-thiol interchange activity (Sects. 2.6, 2.7, and 2.8) is most conveniently measured either as activation of scrambled and inactive RNase or from the increase in absorbance at 340 nm from the cleavage of DTDP (Fig. 2.1c). Production of superoxide as is characteristic of the age-related NOX proteins (Chap. 9) is estimated from the reduction of ferricytochrome c (Fig. 2.1d).

2.1 Spectrophotometric Assay of NADH Oxidase

NAD(P)H oxidase activity with NAD(P)H as substrate is determined from the disappearance of NAD(P)H measured at 340 nm in a reaction mixture of 25 mM Tris-Mes buffer (pH 7.2), 1 mM KCN, and 150 μM NADH at 37 °C and continuous stirring (Morré et al. 1995b) using Hitachi U3210 UV–visible (Hitachi Instruments, San Jose, CA) or SLM Aminco DW2000 (Milton Roy Company, Rochester, NY) spectrophotometers, the latter in the dual wavelength mode of operation with continuous recording or a comparable instrument. While these instruments are capable of recording data electronically, chart recorder output has been the preferred means of equipment use. The instruments were employed in double-beam (Hitachi U3210) or dual wavelength (SLM 2000 with reference at 430) modes with the reference path empty. Data were recorded continuously over intervals of 1 or 5 min each for periods of up to 90 min. For measurements of 1.5-min intervals, rates are monitored continuously over 1 min. After each 1-min measurement interval, the chart paper is returned to the starting position, the baseline is offset by a convenient increment, and recording restarted exactly 1.5 min after initiation of the previous trace. If timing is digital, uncertainty in restart interval is likely less than 1 s and there is no cumulative timing error. When paired instruments were employed, they were directly adjacent to each other and shared a common timer and thermostated water bath. Assays are normally initiated by addition of enzyme. ENOX activities can be measured conveniently with whole cells as NAD(P)H are impermeant substrates.

Circulating water bath temperatures are normally set to 37 °C for mammalian cells and 25 °C for plant cells and tissues. Cuvettes were typically at room temperature when loaded and temperature equilibrated up to 20 min before beginning the assays.

It is important that all reactants be equilibrated at the spectrophotometers' temperature prior to measurement of the oscillatory patterns. During temperature equilibration, sample warming contributes significantly to absorbance values. Near 34 °C, the mean temperature used, a 1° change in temperature results in a density change of 0.03 % (Lide 1992). For turbid samples ($A \cong 1$), this corresponds to an absorbance change of 3×10^{-4}.

For ENOX assays, a grating instrument with an end-on window photomultiplier tube along with the double beam stability offered by this type of instrument is preferred and, with turbid preparations, is essential. For example, the smooth signal generated by the Aminco SLM 2000 offers an unequivocal demonstration of oscillatory behavior with continuous tracings and an opportunity for unambiguous fitting of line slopes to discontinuous traces.

Diode array instruments are excellent for scanning. Full spectrum incident light is selectively absorbed by the sample and transmitted. However, for situations other than for clear aqueous samples of 1 cm path length, their utility is limited. With ENOX proteins it is rarely possible to provide a clear sample. Even highly purified ENOX preparations tend to aggregate and become turbid. With a turbid sample, polychromatic light is scattered. The transmitted light is no longer focused and may not even reach the detector. Within a conventional diode array instrument, the sample

is placed too far from the detector to avoid serious interference from light scatter (see Sect. 2.3.1).

Unfortunately, spectrophotometers of the Aminco SLM 2000 design are no longer available commercially. A comparable instrument with an end-on photomultiplier and dual beam stability is the Spectronics UV 500 (Thermo Electron Scientific Instruments, Rochester, NY). This instrument, appropriately modified to achieve both stirring and temperature control, should fulfill the basic requirements for either continuous or discontinuous measurements of ENOX activities.

Unlike chemical oscillators (Scott 1994), ENOX oscillations are inherent in the protein itself and the period length is not dependent on the chemical environment or temperature per se (period length is independent of temperature). These factors, however, do influence absolute reaction rates and consequently, resolution. However, the greatest contributors to a lack of resolution are turbidity and particle settling. Stirring is essential to eliminate the latter. Turbidity is difficult or impossible to eliminate in most ENOX preparations. Improved resolution with the SLM DW2000 derives from minimization of turbidity influences by the end on photomultipliers. Double beam dual wavelength with A_{430} reference subtraction from the same cuvette to reduce the turbidity component is an aid with very turbid samples but most of the data generated have utilized only a single wavelength. A reference in the reference cell lacking NADH, for example, only exacerbates the turbidity problem so that the routine reference of choice is air. Turbidity may arise from vesicles (membrane preparations), lipid micelles (disrupted vesicles), and protein aggregates (solubilized and purified ENOX proteins). Purified ENOX proteins tend to aggregate to form insoluble (and inactive) amyloid rods under most standard conditions of assay (del Castillo-Olivares et al. 1998; Kelker et al. 2001). Addition of detergent is of limited benefit and may actually aggravate the situation since detergents enhance aggregation of ENOX proteins (Morré et al. 1998e), a phenomenon also encountered with prions (Prusiner et al. 1983).

2.2 Statistical Analysis

From the rate data, period lengths may be verified by fast Fourier analysis. One method for statistical validation of the reproducibility of rate data is time series analysis (Foster et al. 2003). In time series analyses, decomposition fits compare successive oscillatory patterns of period length determined by Fourier analysis (Fig. 1.6b). The decomposition fits (Fig. 1.6c) serve to evaluate the reproducibility of the oscillatory patterns by generating a predicted or forecasted oscillatory pattern and by comparison to the predicted pattern to yield mean average percentage error (MAPE), a measure of the periodic oscillation, mean average deviation (MAD), a measure of the absolute average deviations from the fitted values, and mean standard deviation (MSD), the measure of standard deviation from the fitted values (Foster et al. 2003). A trend line is first fitted to the data. The data are then smoothed by subtracting a centered moving average of length equal to the length of the period

determined by Fourier analysis. Finally, the time series are decomposed into periodic and error components. The decomposition fits are used to validate the periodic oscillatory pattern and to demonstrate that minor intervening fluctuations also recurred within each period as part of a reproducible pattern. The decomposition fits used MINITAB®, a statistical package.

Implicit in the need to visualize periodic oscillations in ENOX activity is a high degree of synchrony. Unsynchronized ENOX preparations as a population would not generate discernable oscillations with a regular period. However, such populations, once synchronized, will generate oscillations under the same identical chemical and thermal conditions as for the unsynchronized preparations (Morré et al. 2002a, b).

2.3 Data Reduction Methods

From the SLM Aminco DW2000 and Hitachi U3210 spectrometers, reaction rate was determined from the least squares linear slope of the absorbance vs. time chart data. In practice this was accomplished by measuring rise vs. run of the linear absorbance vs. time line best fitting the data. Typically, slopes were >10 absorbance standard deviations/min for the SLM Amico DW2000 and normally >3 absorbance standard deviations/min for the Hitachi U3210. Despite the fact that some slopes were within the noise envelope of the traces especially with the Hitachi U3210, slopes were estimated to an accuracy of ±0.015 nmol/min compared to the actual rates recorded at 1–10 nmol/min.

Figure 2.2a is a continuous trace of a well-synchronized single culture of CHO cells determined over 84 min using the Aminco SLM 2000 spectrophotometer to illustrate the oscillatory activity characteristic of the ENOX enzymes from a continuous trace. Intervals of rapid activity were interspersed with intervals of lesser activity. The period length was about 24 min.

No oscillations were observed with NADH alone in the absence of cells (Fig. 2.2b) or with cells alone in the absence of NADH (Fig. 2.2c). In the absence of cells, a slow rate of non-enzyme-catalyzed NADH oxidation was observed. In the absence of NADH, the absorbance increase was due to light scattering as turbidity increased.

The continuous tracings provided by the Aminco SLM DW2000 and Hitachi U3210 recording spectrophotometers have been analyzed variously to elucidate details of the oscillatory patterns. One method developed over several years of experimentation is to estimate rates from line slopes fitted to continuous traces obtained over 1 min at 1.5-min intervals. The 0.5-min intervals between measurements are sufficient to allow for chart repositioning and instrument restart. The rise over run ratio allows for accurate measurement of slopes determined over 1 min with a precision of ±0.015 nmol, approximately equivalent to instrument and/or thermal variation (variation in trace width) for the Aminco SLM DW2000. The actual rates estimated were in the range of 1–10 nmol/min, 50–500 times the

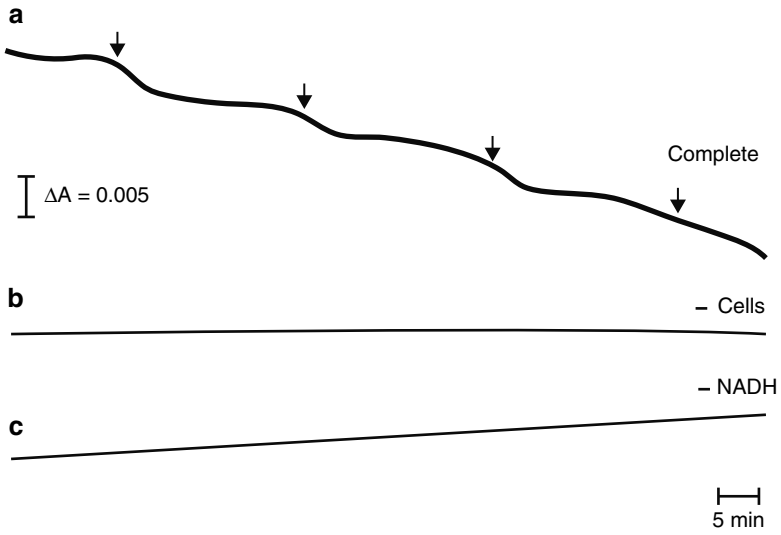

Fig. 2.2 A continuous trace of the decrease in A_{340} as recorded using an Aminco SLM 2000 spectrophotometer in the dual wavelength mode of operation as a measure of consumption of NADH over 96 min for a well-synchronized (by light exposure) culture of CHO cells. (**a**) Complete reaction mixture. Periods of rapid oxidation of NADH alternate with periods of much slower NADH oxidation. (**b**) Reaction mixture lacking cells. (**c**) Reaction mixture lacking NADH. Reproduced from Morré and Morré (2003c) with permission of International Hormesis Society

precision with which the line slopes were determined. This ratio represents the power of the line slope method of minimizing instrument or thermal variation as a significant source of measurement error. Maxima and minima are readily discerned and data are obtained that permit statistical evaluations not possible from continuous traces. For example, the maxima in NADH oxidation of well-synchronized preparations frequently may be resolved into two maxima rather than a single maximum. In addition, minor oscillations coinciding with maxima in protein disulfide-thiol interchange also may be discerned (Sun et al. 2000).

Oscillations in the rate of oxidation of NADH by CHO cells illustrated in Fig. 2.3 also with a period length of 24 min become more obvious when analyzed over 5 min (Fig. 2.3a, b) or over 1 min at intervals of 1.5 min (Fig. 2.3c, d) using the Aminco SLM 2000 in the dual wavelength of operation with reference at 430 nm. Both measuring and reference wavelengths pass simultaneously through the same cuvette so that errors due to electronic fluctuation and turbidity changes, for example, are minimized. Panel A illustrates rates determined over 5 min as would be done for an average determination of specific activity. Since the rates were not steady state, rates from a number of such traces (usually 2–5) normally were averaged where determination of an average rate is a primary consideration. With 5-min traces linked front to back, the oscillatory pattern shown in (b) was revealed which was similar to that observed with the continuous recording shown in Fig. 2.2a.

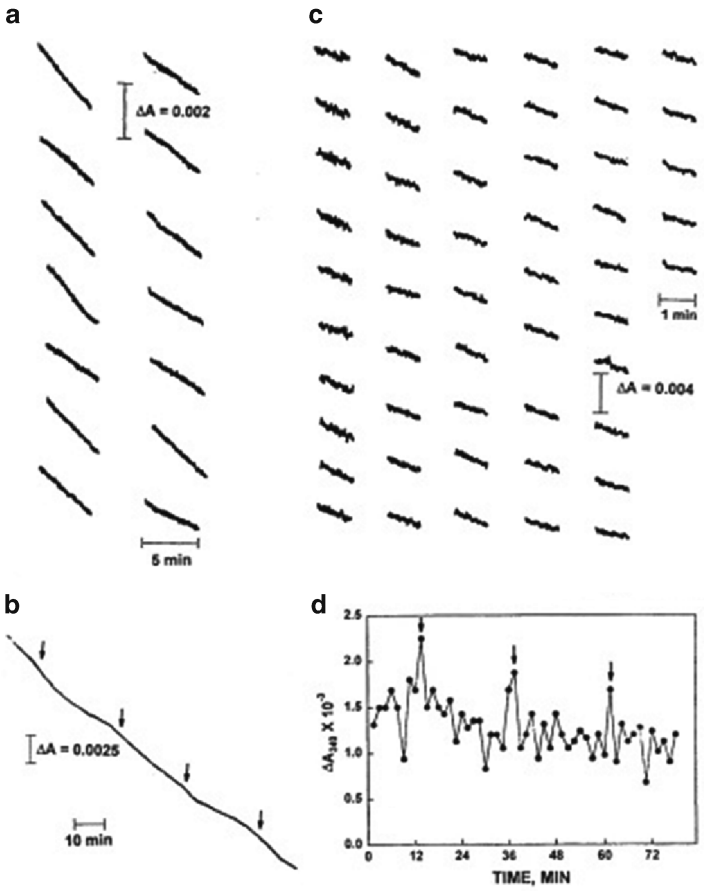

Fig. 2.3 Oscillatory oxidation of NADH by 10^6 CHO cells as in Fig. 2.2 (Aminco SLM 2000) illustrating three methods of spectroscopic analyses employed to demonstrate oscillations. (**a**) Activity analyzed for successive intervals of 5 min each. Traces are arranged from *top* to *bottom* and from *left* to *right* (see Fig. 2.3d). (**b**) The 5-min assays aligned as a continuous trace. (**c**) Activity analyzed over 1 min at intervals of 1.5 min. Traces are arranged from *top* to *bottom* and from *left* to *right* (see Fig. 2.3d). (**d**) Slopes calculated from (**c**). Assays were for 70 min. The period length was 24 min (*arrows*). HeLa cells contain a background activity approximately equal to that of the oscillatory activity that is proteinase K susceptible and does not oscillate. Reproduced from Morré and Morré (2003c) with permission of International Hormesis Society

For more detailed evaluations, determinations of rates over 1 min at intervals of 1.5 min are illustrated in Fig. 2.3c. The measured slopes when represented graphically in Fig. 2.3d illustrate maxima separated by intervals of 24 min. With the SLM 2000, the width of the trace was such that when slopes were estimated to the nearest 0.1 mm, measurement errors were ±0.015 nmol/min. Measurement errors greater than ±1 mm (±0.05 nmol/min) would have been virtually impossible to introduce. These assays all were for 70 min. HeLa cells contained a background activity as seen in

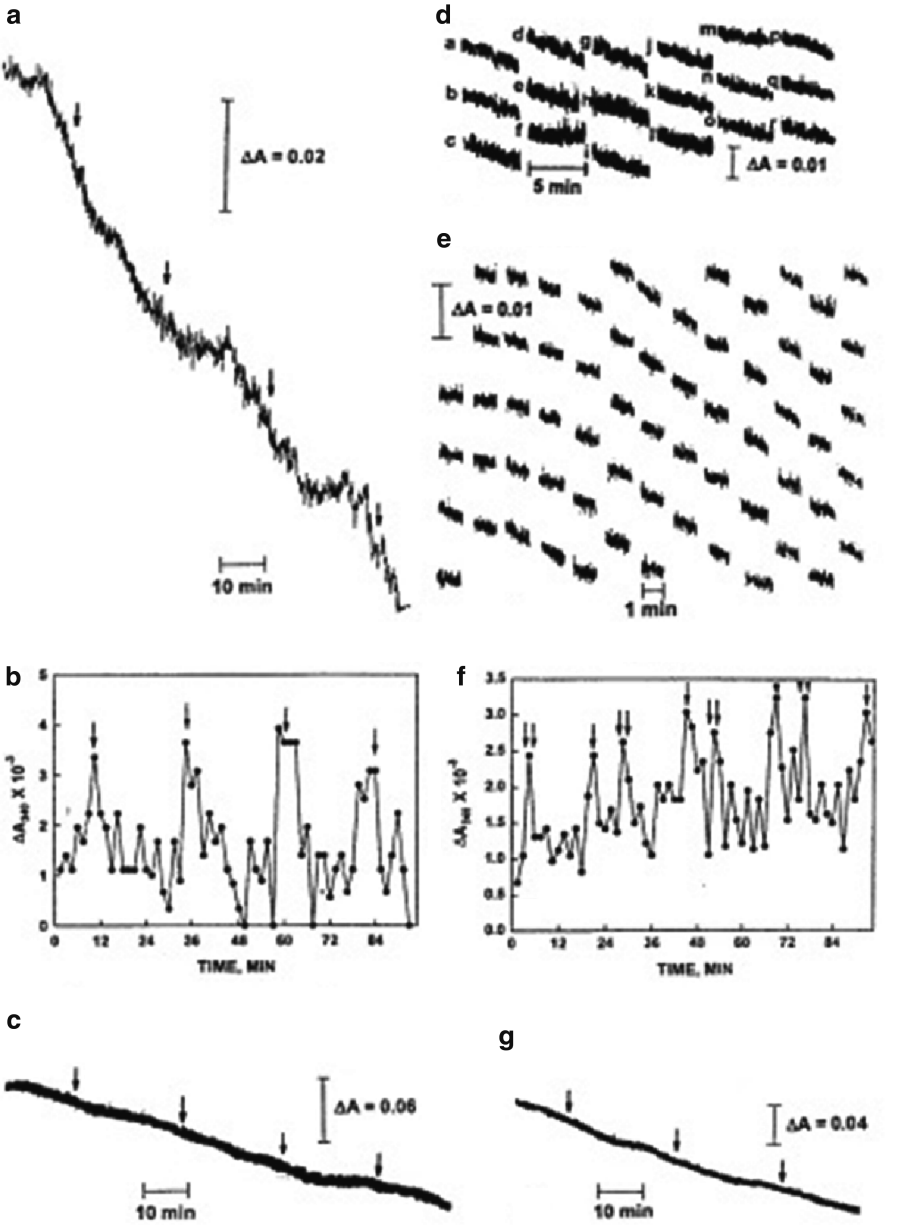

Fig. 2.4 Oxidation of NADH by a crude preparation of isolated, intact plasma membrane vesicles from soybean measured using paired Hitachi U3210 dual beam spectrophotometers with air as reference illustrating typical oscillatory patterns. The solutions were very turbid (initial absorbance of 1.4) and represent a worst-case scenario at the limits of the capacity of the photospectrometer. (**a**) Continuous trace over 90 min with alternating rapid and slow rates of NADH oxidation. (**b**) An identical aliquot of the same preparation as in (**a**) but analyzed in parallel using

Fig. 2.3d approximately equal to that of the oscillatory activity. The background activity was susceptible to digestion with proteinase K and did not oscillate (Morré and Morré 2000). The oscillatory ENOX activities are resistant to protease digestion, including digestion with proteinase K (del Castillo-Olivares et al. 1998).

A double peak oscillatory pattern is also typically observed as illustrated with plasma membranes from stem sections of dark-grown soybean seedlings analyzed using the SLM 2000 (Fig. 2.4). The plasma membranes were solubilized with 0.5 % Triton X-100 to minimize turbidity. Detergent treatment, however, introduced a non-oscillatory background NADH oxidase activity nearly equal to the oscillatory NADH activity. The background activity introduced by detergent treatment derives from the inner surface of the solubilized plasma membrane vesicles (Morré and Morré 2000) and is removed by digestion with proteinase K. These preparations were well synchronized by light treatment of the soybeans prior to harvest of the plant material and show two maxima in NADH oxidase activity with the second maximum (double arrow) following the first (single arrow) by about 6 min (Fig. 2.4f).

Much of the previous work, especially with plants, compared measurements using two side-by-side Hitachi U3210 dual beam spectrophotometers with air as reference. The most challenging measurements were with turbid untreated preparations of plasma membrane vesicles (initial absorbances between 1 and 2). Continuous traces exhibited more noise than those with the SLM 2000. Figure 2.5a, b compare a continuous trace of soybean plasma membranes with a starting absorbance of 1.4 generated in one of the two machines with data obtained from analyses of individual rates determined over 1 min at 1.5-min intervals in (b) as illustrated in (e). A regular pattern of rapid rates alternating with very slow rate was observed with both data sets. These intact plasma membranes have a very low background rate and the rate of NADH disappearance in between the maxima actually reached zero (Fig. 2.4b). Panel (c) illustrates a series of 18 5-min traces assembled end to end for the same plasma membrane preparation assayed in one of the two machines subsequent to the data of (a) and (b) but timed to be in phase. The individual traces are shown in (d). The sequence with which the traces were acquired is given by the letters a–r. The same sequence was followed for Figs. 2.3a, c and 2.4e (top to bottom, left to right). These types of traces are those most commonly used to measure effects of inhibitors and other parameters affecting ENOX activities. Examples of sequential 5-min assay segments where activity in m and f exhibits little or no activity are encountered as well (Fig. 2.3c). A minimum also is encountered at the end of i and the

Fig. 2.4 (continued) the second Hitachi instrument based on rates determined over 1 min at 1.5-min intervals. (**c**) An assembly of 18 assays of NADH oxidation each over 5 min determined on the same preparation sequentially but in phase with (**a**) and (**b**). (**d**) Examples of 5-min traces used in the generation of (**c**). These preparations, largely lacking background activity and relatively well synchronized by light, exhibit periods where activity slows or stops between periods of rapid activity. The period length is 24 min. The 5-min assay segments labeled f and m exhibit little or no activity. A minimum is also encountered at the end of i and the beginning of j. (**e**) Examples of rates determined over 1 min at intervals of 1.5 min. (**f**) Analyses of (**e**). (**g**) Sequential 5-min traces as in (**d**) except determined sequentially without interruption. All assays were for 90 min

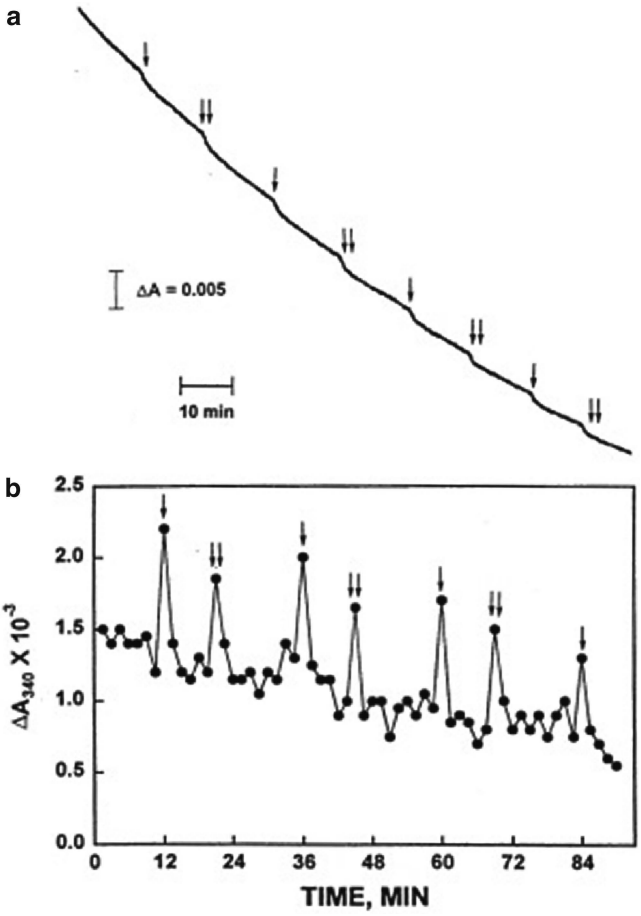

Fig. 2.5 Oxidation of NADH by a well-synchronized preparation of soybean plasma membranes solubilized in Triton X-100 to reduce turbidity also using the Aminco SLM 2000 in the dual wavelength mode of operation showing two distinct activity patterns (single and double arrows). (**a**) Continuous trace over 108 min. (**b**) Activity analyzed over 90 min from slopes determined over 1 min at 1.5-min intervals as illustrated for Fig. 2.3c, d. Since the vesicles were solubilized, a major contribution to background comes from a NADH oxidase of the internal plasma membrane surface that does not oscillate (Morré and Morré 2000). Reproduced from Morré and Morré (2003c) with permission of International Hormesis Society

beginning of j which would be detected with 1-min traces as a rate near zero. Figure 2.4e gives examples of sequential 1-min traces measured at intervals of 1.5 min as for Fig. 2.4b, f. Despite the width of the traces, slopes even with these relatively turbid samples were determined with an accuracy and reproducibility sufficient to reliably reveal details of the oscillatory pattern (Fig. 2.4b). A further illustration is provided in Fig. 2.4f, g where the two instruments again were used in parallel. Figure 2.4f shows the results of the 1-min analyses at intervals of 1.5 min whereas in (g), the same preparation was analyzed based on 18 consecutive 5-min

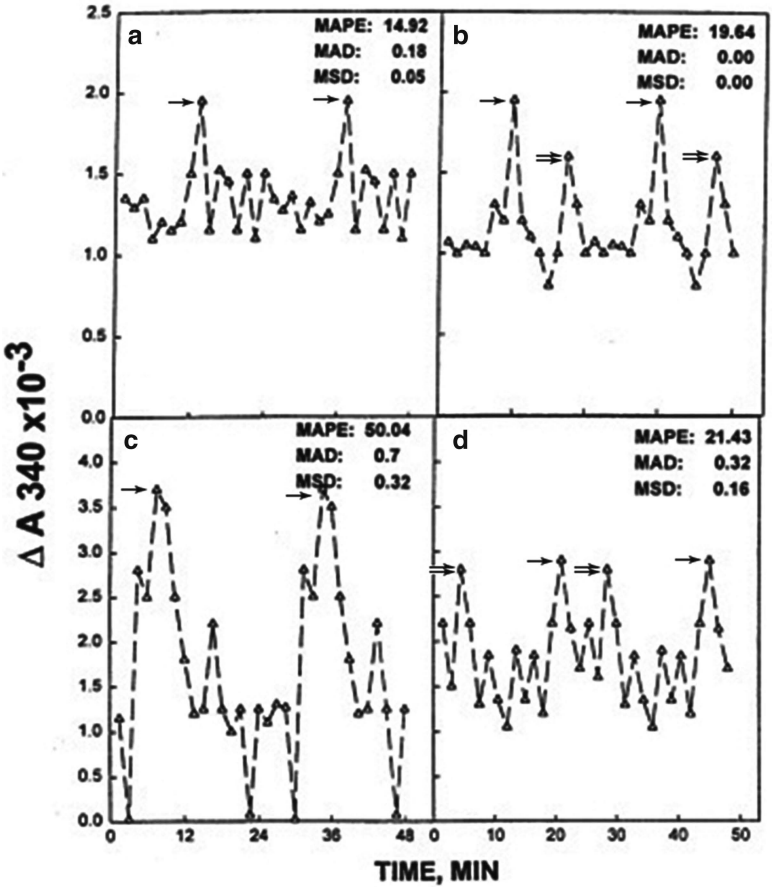

Fig. 2.6 Decomposition (time series) analyses of the oscillatory patterns of NADH oxidation of Figs. 2.3, 2.4, and 2.5. (**a**) Decomposition fit of data of Fig. 2.3d. The data consist of a pattern of repeating oscillations, all conforming to a 24-min period length (*arrows*). (**b**) Decomposition fits (*open symbols, dashed lines*) for two full cycles of data of Fig. 2.5b. (**c**) Decomposition fits for data of Fig. 2.4b. (**d**) Decomposition fits for data of Fig. 2.4f. Period lengths were determined by Fourier analysis. The decomposition fits show the reproducibility of the patterns of oscillations. Three measures of the accuracy of the statistically fitted values are provided in the *insets.* Reproduced from Morré and Morré (2003c) with permission of International Hormesis Society

scans as in (c) and (d) except that the rates were determined sequentially without interruption. Both methods revealed a similar pattern of oscillations.

To illustrate the reproducibility of the pattern of oscillations, decomposition fits for two full periods of each of the experiments of Figs. 2.3d, 2.4b, f, and 2.5b are shown in Fig. 2.6 along with three measures of the accuracy of the statistically fitted values. The MSD comparing all four data units analyzed averaged 13 %. Differences between maxima and minima were highly significant ($p < 0.001$). Also evident from the decomposition fits were the double-peak pattern of Fig. 2.4f (Fig. 2.5b) compared to the single-peak patterns of Fig. 2.3d.

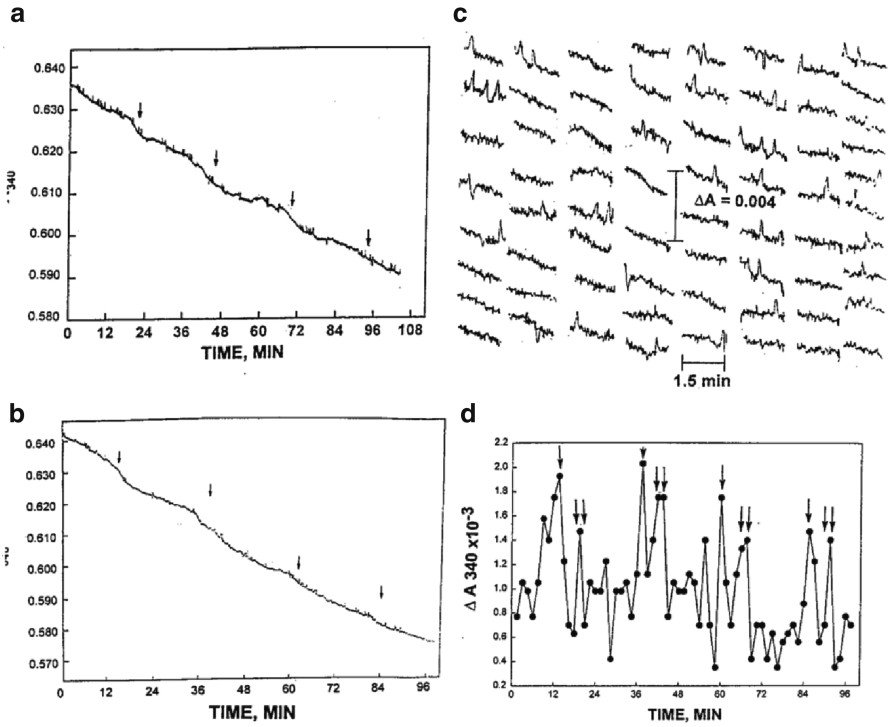

Fig. 2.7 Decrease in A_{340} from the oxidation of NADH measured using the Spectronics UV 500 spectrophotometer. (**a**) Continuous trace over 105 min of a preparation containing 10^6 intact CHO cells where synchrony was achieved by addition of 1 μM melatonin at $t = 12$ min. *Arrows* spaced at 24 min coincide with intervals where rapid rates of NADH oxidation were observed. (**b**) As in (**a**) except for a preparation of plasma membranes of dark-grown soybean hypocotyls (150 mg total protein). Melatonin (1 μM) was added at $t = 12$ min. (**c**) Data of (**b**) displayed as successive 1.5-min segments. (**d**) Analysis of (**c**) giving rates determined by least squares analyses of the 1.5-min segments shown in (**c**). Reproduced from Morré and Morré (2003c) with permission of International Hormesis Society

Absorbance values recorded at intervals of 10 sec using the Beckman DB200 spectrophotometer (Beckman Instruments, Palo Alto, CA) also provided useful information (Fig. 2.7). These data were analyzed to determine best fit slopes at intervals of 1.5 min. Oxidation was calculated from the formula $N-(N+1)$ for each 1.5-min interval to generate data comparable to that of Fig. 2.4f.

2.3.1 Diode Array Instruments

With assay of A_{340} from diode assay instruments, the variation in ratios normally fall within the envelope of machine variation, even with preparations treated with detergents such as Triton X-100 to reduce light scattering (Fig. 2.8). Thus, with the

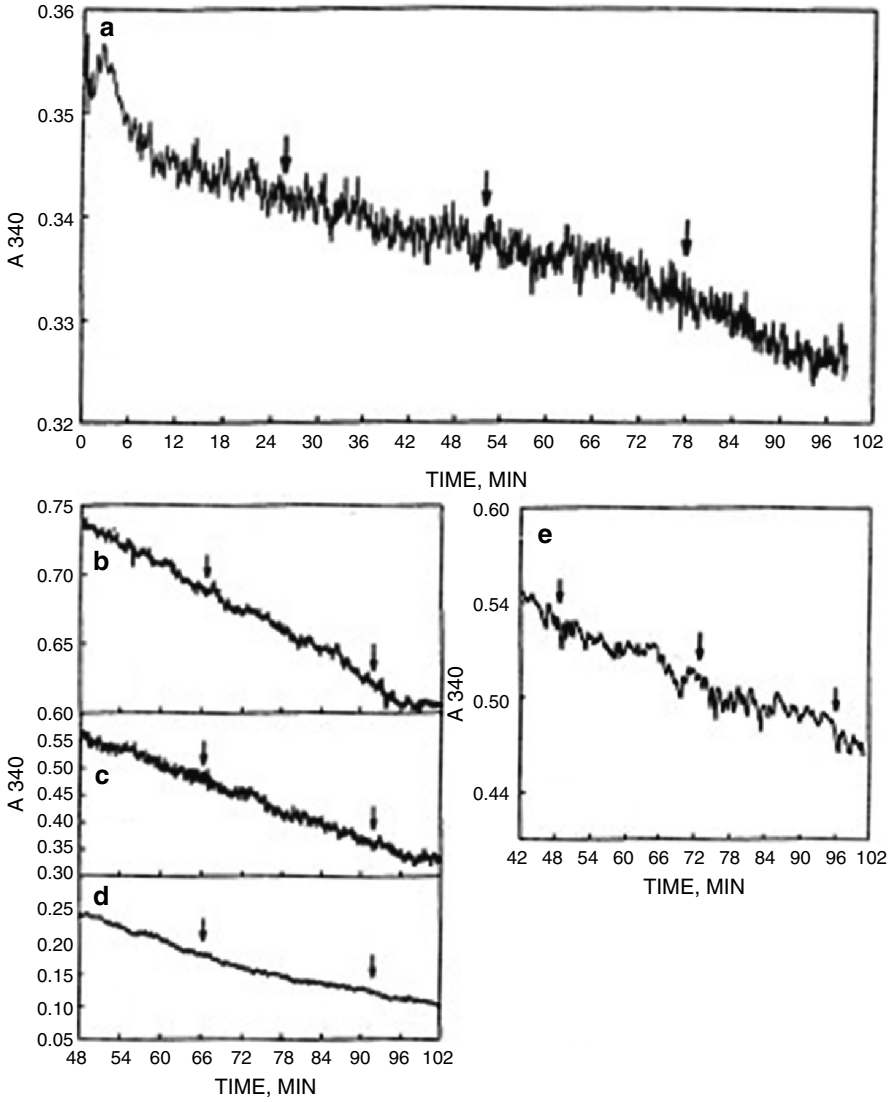

Fig. 2.8 Comparable assays of the decrease in A_{340} due to NADH oxidation using a diode array spectrophotometer (HP8452A). *Arrows* are spaced at 24 min to coincide with at least one interval where rapid rates are separated by a slow rate. (**a**) CHO microsomes dissolved in 0.5 % Triton X-100 to reduce turbidity. (**b**–**d**) Three different preparations of CHO membranes in which synchrony was induced by addition of l μM melatonin at $t=0$. (**d**) With 5 % Triton X-100 added followed by centrifugation to remove floating lipids. A double peak with a 24-min period similar to that of Fig. 2.3 was seen at the *arrows* in all three repetitions on subsequent days with different preparations. (**e**) A skunk cabbage (*Symplocarpus foetidus*) spadix plasma membrane preparation comparable to the soybean plasma membrane preparation of Fig. 2.3a. Reproduced from Morré and Morré (2003c) with permission of International Hormesis Society

Hewlett Packard 8452 single beam diode array spectrophotometer, variations due to light scatter, even in well-synchronized preparations, were sufficient to prevent observation of statistically significant deviations in reaction rates of the continuous traces that would distinguish them from single experiential or linear decay (Fig. 2.8). When the diode array data were numerically differentiated using the Savitsky–Golay algorithm presuming local linearity and with averaging times ranging from 11 to 121 s (Savitsky and Golay 1964), no departures from linearity could be discerned above the variations due to light scatter. At least six different single beam diode array instruments have been evaluated and compared with outcomes similar to those observed with the Hewlett Packard 8452 instrument.

2.4 Measurement of Hydroquinone Oxidase Activity with Reduced Coenzyme Q_{10} or Phylloquinone as Substrate

Hydroquinone oxidase activity may be estimated as for NADH except from absorbance changes at 275 nm, 410 nm or both with reduced coenzyme Q_{10} (Tishcon, Westbury, NY) (Kishi et al. 1999) or reduced phylloquinone (Bridge et al. 2000) as the substrate (Fig. 2.9).

2.4.1 Enzyme Assay for Reduced Coenzyme Q_{10} Oxidase

The method for preparation of reduced coenzyme Qs (50 mM coenzyme Q_0 stock solution or 7.5 mM coenzyme Q_{10} stock solution in ethanol) involved addition of an equal volume of 0.25 % $NaBH_4$ under nitrogen followed after several min by 0.1 vol. of 0.1 N HCl to degrade the excess $NaBH_4$. The colorless solution held at room temperature must be prepared fresh for each experiment.

For oxidation of $Q_{10}H_2$ the reaction mixture contained the enzyme source, in 2.5 mL of 50 mM Tris-Mes buffer, pH 7.0. Triton X-100 (0.08 %) was used to solubilize the $Q_{10}H_2$ in the assay buffer. The reaction was started with the addition of 40 μL of 5 mM $Q_{10}H_2$. An extinction coefficient of 0.805/mM/cm was used to calculate the rate of $Q_{10}H_2$ oxidation (Sun et al. 1995). Rate measurements are illustrated for continuous traces (Fig. 2.10) as well as over 1 min at 1.5-min intervals (Fig. 2.11).

Q_{10} in ethanol exhibits a maximum at 275 nm, a broad band at about 410 nm, and a minimum at 236 nm (Crane et al. 1957; Fig. 2.9). Upon reduction of the quinone, the bands at 275 and 410 nm disappear and a new peak characteristic of $Q_{10}H_2$ appears at 290 nm (Hatefi 1963) shown schematically in Fig. 2.1.

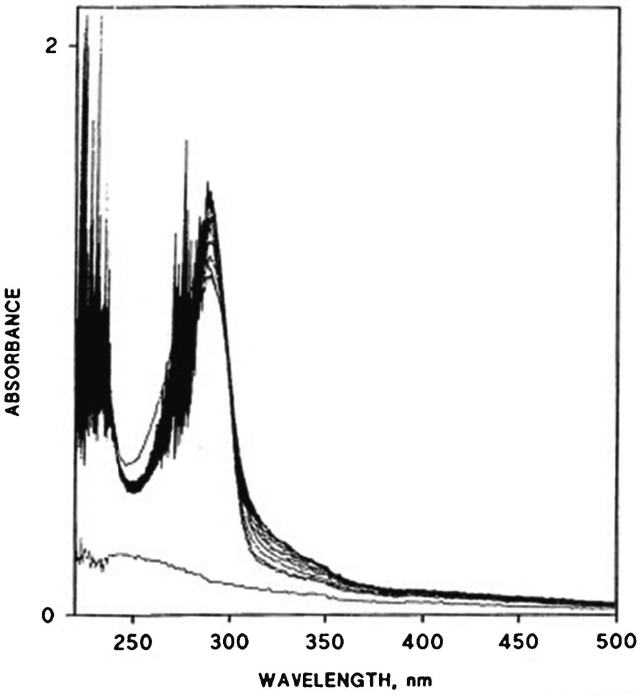

Fig. 2.9 Oxidation of $Q_{10}H_2$ (0.2 mM) in the presence of 0.2 mM Q_0. The preparation contained 0.6 mg protein, 1.2 mM EDTA, 0.08 % Triton X-100 and 50 mM Tris-Mes buffer, pH 7.0, and was scanned every 5 min for 50 min. Oxidation of $Q_{10}H_2$ is indicated by the increase in absorbance at 410 nm accompanied by a decrease in absorbance at 290 nm as illustrated diagrammatically in Fig. 2.1b. Reproduced from Kishi et al. (1999), Copyright 1999 with permission of Elsevier

2.4.2 Enzyme Assay for Reduced Phylloquinone Oxidase

For oxidation of reduced phylloquinone (Bridge et al. 2000), the reaction mixture contained 2.5 mL of 50 mM Tris-Mes buffer, pH 6.5. The reaction was started by the addition of 40 μL of the reduced 20 mM phylloquinone. The reduced phylloquinone oxidase activity was measured spectrophotometrically at a wavelength of 410 nm at 27 °C as described by Sun et al. (1995) for reduced coenzyme Q_{10} using a Hitachi U3210 spectrophotometer. A blank rate was subtracted in which the assay was carried out in the absence of added proteins. The extinction coefficient used for K_1H_2 oxidation was 0.74/mM/cm. The oscillatory pattern of K_1H_2 oxidation is illustrated in Fig. 2.12.

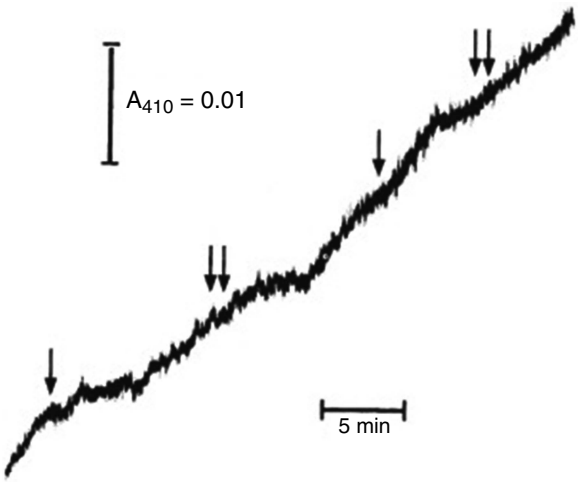

Fig. 2.10 Oxidation of $Q_{10}H_2$ as determined from the increase in absorbance at 410 nm monitored with an Aminco SLM 2000 in the dual wavelength mode of operation. The enzyme source was a solubilized and partially purified ENOX preparation from the surface of human cervical carcinoma (HeLa) cells that contained both ENOX1 (24-min period) and ENOX2 (22-min period). Periods of rapid oxidation (*arrows*) of $Q_{10}H_2$ (Tishcon, Westburg, NY) alternate with periods of much slower $Q_{10}H_2$ oxidation. The *single arrows* are separated by 24 min, whereas the *double arrows* are separated by 22 min. Results where $Q_{10}H_2$ oxidation was monitored from the decrease in A_{290} were similar. Reproduced from Morré (2004), Copyright 2004 with permission of Elsevier

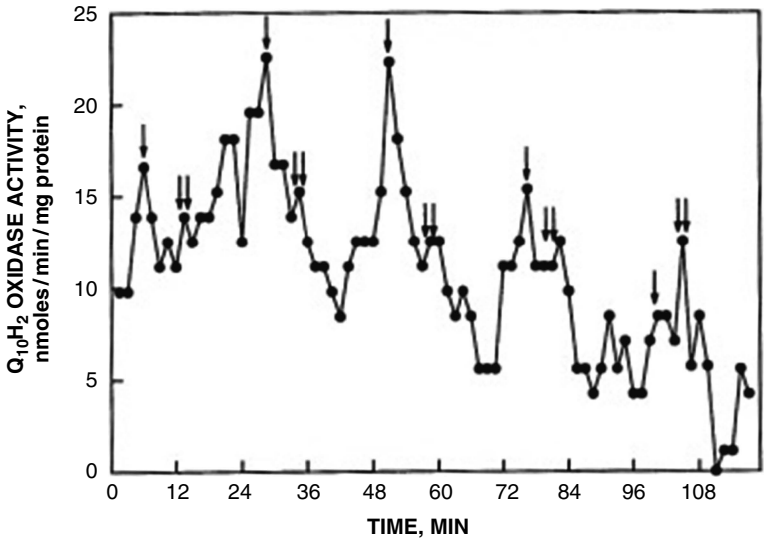

Fig. 2.11 Rate measurements over 1 min at 1.5-min intervals to illustrate the periodic variation in the rate of oxidation of $Q_{10}H_2$ as a function of time over 114 min. The enzyme source was a solubilized and partially purified ENOX preparation from the surface of human cervical carcinoma (HeLa) cells that contained both ENOX1 (24-min period length, *single arrows*) and ENOX2 (22-min period length, *double arrows*). Reproduced from Kishi et al. (1999), Copyright 1999 with permission of Elsevier

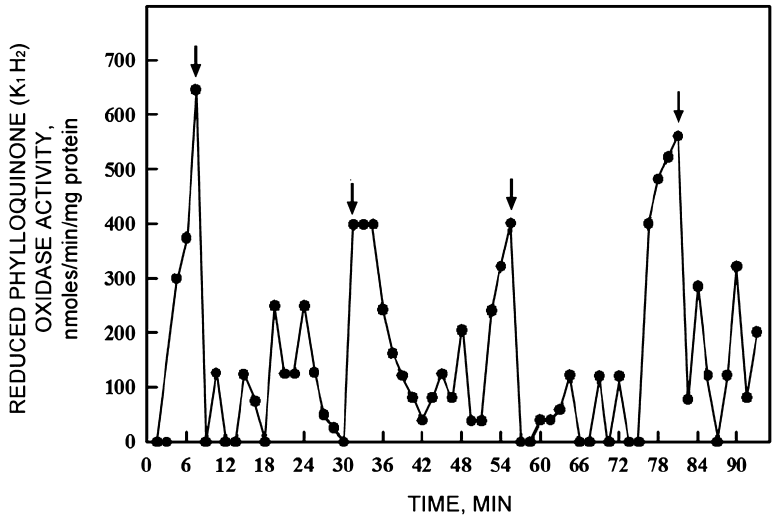

Fig. 2.12 Periodic variation in the rate of oxidation of reduced phylloquinone (K_1H_2) (0.32 mM) as a function of time over 93 min showing four maxima (*arrows* at 7.5, 31.5, 55.5, and 79.5 min) for an enzymatic preparation enriched in NADH oxidase activity solubilized from isolated plasma membrane vesicles. The average period length was about 24 min. The concentration of phylloquinone was 0.32 mM, the pH was 7, and the protein amount was 35 μg/assay. Values are from a single experiment. Reproduced from Bridge et al. (2000), Copyright 2000 with permission of Elsevier

2.5 Dissolved Oxygen Measurement

In our published studies, oxygen was measured using Yellow Springs Instruments model 53 Clark-type polarographic dissolved oxygen probe fitted with a Yellow Springs Instruments high-sensitivity membrane and electrolyte solution (5.25 g KCl and 63 μL Kodak Photo-Flo in 350 mL of distilled H_2O) connected to an amplifier and placed in a reaction chamber (Orczyk et al. 2005). A steady stream of 37 °C water was pumped through a water jacket surrounding the chamber. In addition, a Micro Stirring Bar, measuring 7 mm in length and 2 mm in diameter, was used to mix the solution. Measurements with a total sample volume of 2.5 mL were recorded with a Kipp and Zonen type BD112 chart recorder set at a rate of 2 mm/min and a scale of 10 mV (Figs. 2.13, 2.14, and 2.15). Assays were in the presence of phosphate-buffered (pH 7.4) saline and 2 mM KCN.

Calibration was based on 100 % air saturated water at 37 °C and 0 salinity (0.1869 mM) as compared to 0 % air saturated water obtained by anhydrous sodium sulfite titration (Clesceri et al. 1998). Instrument traces of oxygen consumption for CHO (Fig. 2.12) and HeLa cells (Fig. 2.13) show the characteristic oscillatory pattern of alternating fast and slow rates. Rates determined by numerical averaging show the oscillatory pattern more clearly (Fig. 2.14).

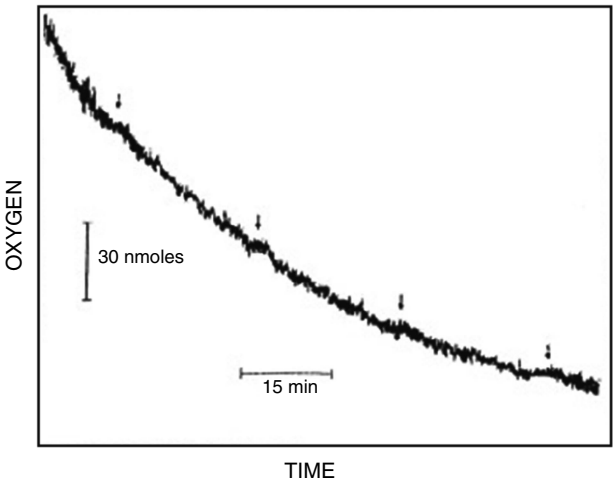

Fig. 2.13 Instrument trace of oxygen consumption by 3×10^7 CHO cells. The rates show a pattern of slow rates separated by rapid rates. *Single arrows* marking slow rates are separated by intervals of 24 min. The assay was in phosphate-buffered (pH 7.4) saline and 2 mM KCN. The initial rate of oxygen consumption was estimated to be 0.2 nmol molecular oxygen/min/10^6 cells. Reproduced from Orczyk et al. (2005) with permission of Springer-International

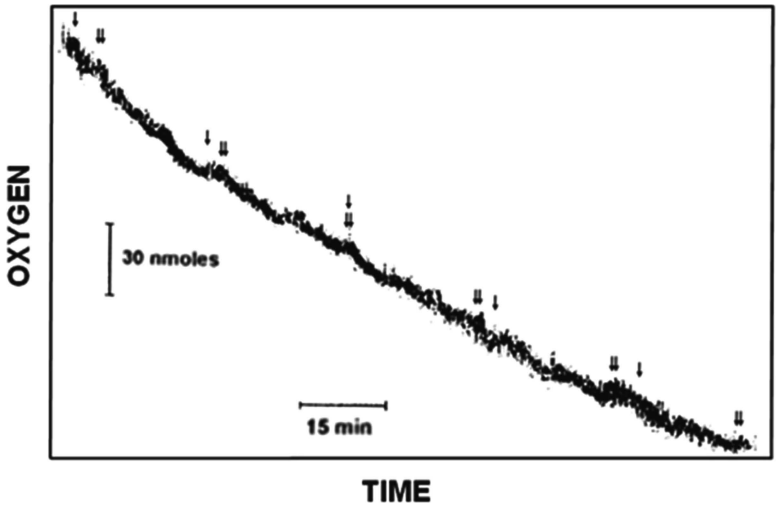

Fig. 2.14 Instrument trace of oxygen consumption by 4×10^7 HeLa cells. The rates show a pattern of alternating slow and fast rates. *Single arrows* marking slow rates are separated by intervals of 24 min characteristic of the constitutive ENOX1. *Double arrows* denote intervals of 22 min characteristic of the tumor-specific, ENOX2 form. Assay was in phosphate-buffered (pH 7.4) saline and 2 mM KCN. Rapid rates of oxygen consumption were estimated to be between 0.15 and 0.2 nmol molecular oxygen/min/10^6 cells. Reproduced from Orczyk et al. (2005) with permission of Springer-International

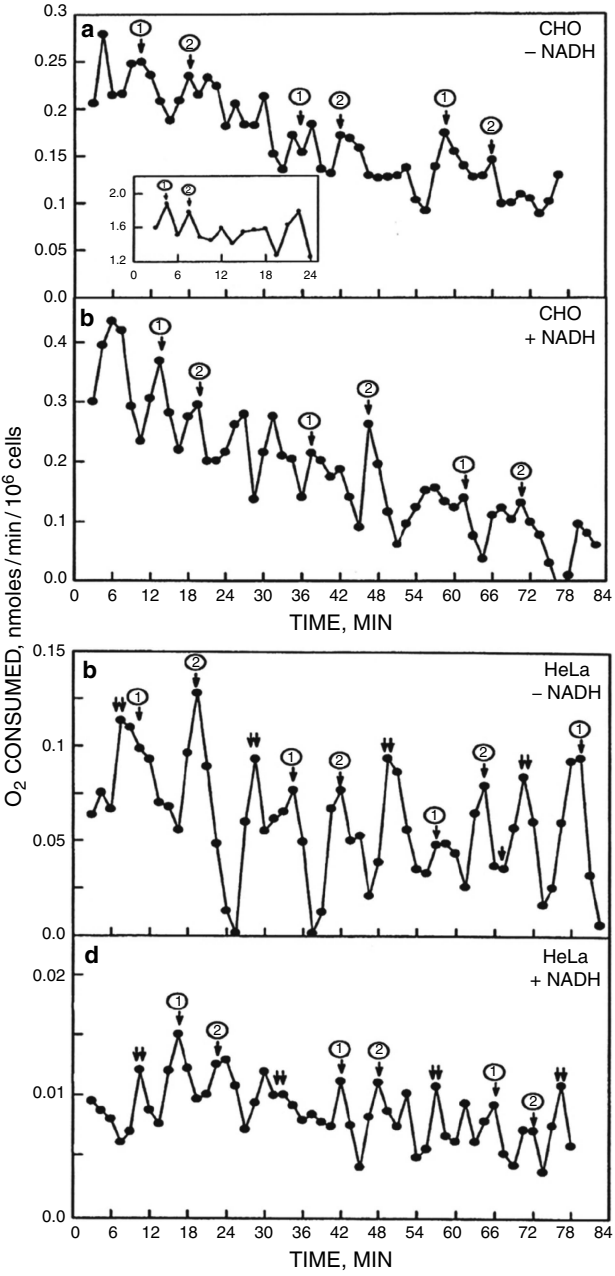

Fig. 2.15 Oxygen consumption measured over 1.5-min intervals by numerical averaging from the cumulative oxygen consumption as illustrated in Figs. 2.13 and 2.14. (**a**, **b**) 2×10^7 CHO cells in the absence (**a**) or presence (**b**) of 150 μM NADH. The *inset* in (**a**) is a decomposition fit of the type used to validate the reproducibility of the recurrent pattern and to provide the three measures of accuracy. The CHO cells exhibit maxima (*arrows* labeled ① and ②) that recur at regular intervals of 24 min as is characteristic of the constitutive ENOX1. (**c**, **d**) 4×10^7 HeLa cells in the absence (**c**) or presence (**d**) of 150-μM NADH. HeLa cells exhibit the maxima labeled ① and ② recur at regular intervals of 24 min as is characteristic of ENOX1 together with a second set of maxima (*double arrows*) separated by 22 min as is characteristic of the cancer-associated ENOX form, ENOX2. The assay was in phosphate-buffered (pH 7.4) saline containing 2 mM KCN. Reproduced from Orczyk et al. (2005) with permission of Springer-International

2.6 Estimation of Protein Disulfide-Thiol Interchange Activity

RNase A activity was assayed by two different methods. In the first method, a spectrophotometric assay based on cCMP as an RNase substrate was used (Lyles and Gilbert 1991) as diagramed in Fig. 2.16–2.18a. Inactive, oxidized, and scrambled (see below) RNase A was incubated together with cCMP in Tris-Mes buffer, pH 6.4, with or without GSH or GSSG. In the absence of a protein disulfide isomerase or protein disulfide-thiol interchange activity, the scrambled RNase was inactive (activity about 2 % that of native RNase). However, in the presence of a protein disulfide isomerase or protein disulfide-thiol interchange activity, the scrambled RNase became active as evidenced by an increase in A_{296} from the RNase-catalyzed hydrolysis of cCMP.

The assay mixture contained 50 mM Tris-Mes buffer (pH 6.0), 0.45 mM cCMP, 1 μM GSH or GSSG or GSH plus GSSG, and 400 μg of plasma membrane protein preincubated at 30 °C for 20 min. The assay was initiated by the addition of scrambled RNase A (see below). Hydrolysis of cCMP resulting from the activation of the initially randomly oxidized and inactive RNase was recorded continuously as an increase in A_{296}. The concentrations of cCMP were determined at a wavelength of 296 nm (extinction coefficient = 0.19/mM/cm). Spectrophotometric measurements were in parallel using two Hitachi (Tokyo, Japan) U3210 spectrophotometers with thermostatic cell compartments maintained at 30 °C with continuous stirring (Figs. 2.16 and 2.18a).

2.7 Preparation of Scrambled RNase Substrate

To prepare the scrambled and inactive RNase substrate, native RNase A (Sigma, type 1-AS from bovine pancreas) (30 mg/mL) was incubated for 1 h at 35 °C in 50 mM Tris-acetate, pH 8.6, containing 9 M urea and 130 mM DTT (Hillson et al. 1984) to denature and reduce the protein.

The denatured and reduced protein was then isolated by adjusting the pH to 4.0 with glacial acetic acid, followed by elution from a column of Sephadex G-25 with degassed 0.1 M acetic acid. The estimation of the protein concentration was followed by spectrophotometric measurement at 280 nm using native RNase A as the standard. The samples were diluted to approximately 0.5 mg/mL with 0.1 M acetic acid. Solid urea was added to the eluted RNase to a final concentration of 10 M, after which 0.1 M sarcosine hydrochloride was added and the pH adjusted to 8.5 with 1 M Tris. The mixture was then incubated in the dark for 2–3 days during which time the denatured protein was randomly oxidized (scrambled). The scrambled product was recovered by acidification of pH 4.0 with glacial acetic acid and elution from Sephadex G-25 in 0.1 M acetic acid. Fractions containing protein were pooled,

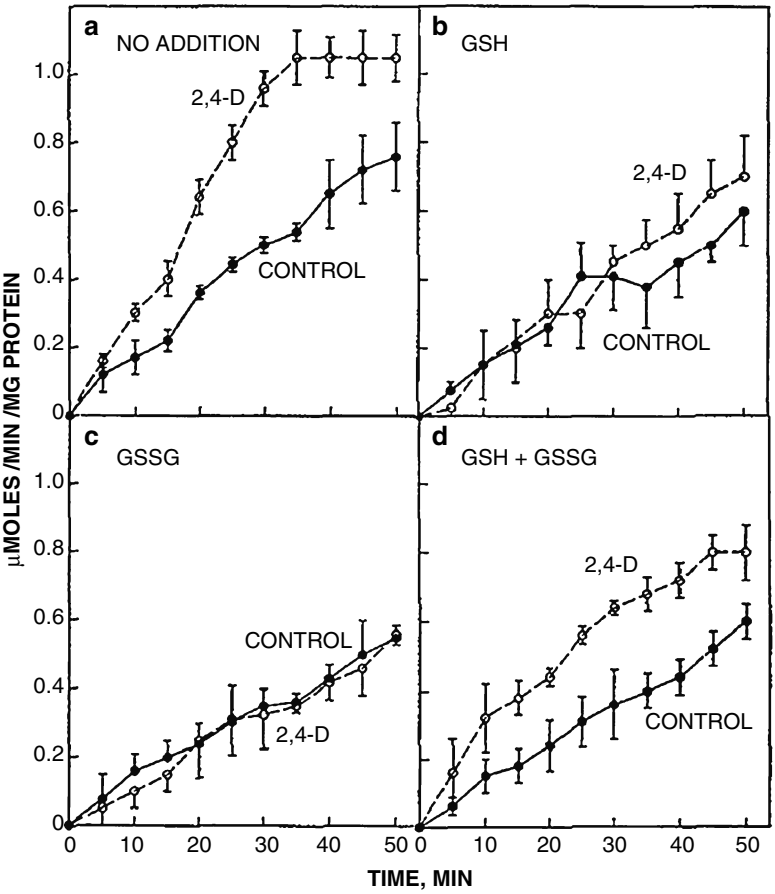

Fig. 2.16 Protein disulfide-thiol interchange activity estimated from the activation of scrambled RNase in the presence of cCMP substrate. Soybean plasma membranes (400 μg) were incubated together with scrambled (inactive) RNase and the cCMP substrate for the times indicated and the specific activity was determined over 5 min at successive 5-min intervals for each preparation. The GSH and GSSG (alone or in combination) solutions were freshly prepared and the final concentrations were 1 μM. The activity was stimulated by the synthetic plant growth hormone, 2,4-dichlorophenoxyacetic acid (2,4-D) at a final concentration of 1 μM. Results are means ± standard deviation of triplicate experiments. Reproduced from Morré et al. (1995d), Copyright 1995 with permission of Elsevier

adjusted to pH 8.0, and stored at 4 °C. Thiol groups, as determined using 5,5′-dithio(2-nitrobenzoic acid) (Ellman 1959) were 80–90 % oxidized.

The preparation of the scrambled RNase substrate is illustrated diagrammatically in Fig. 2.18.

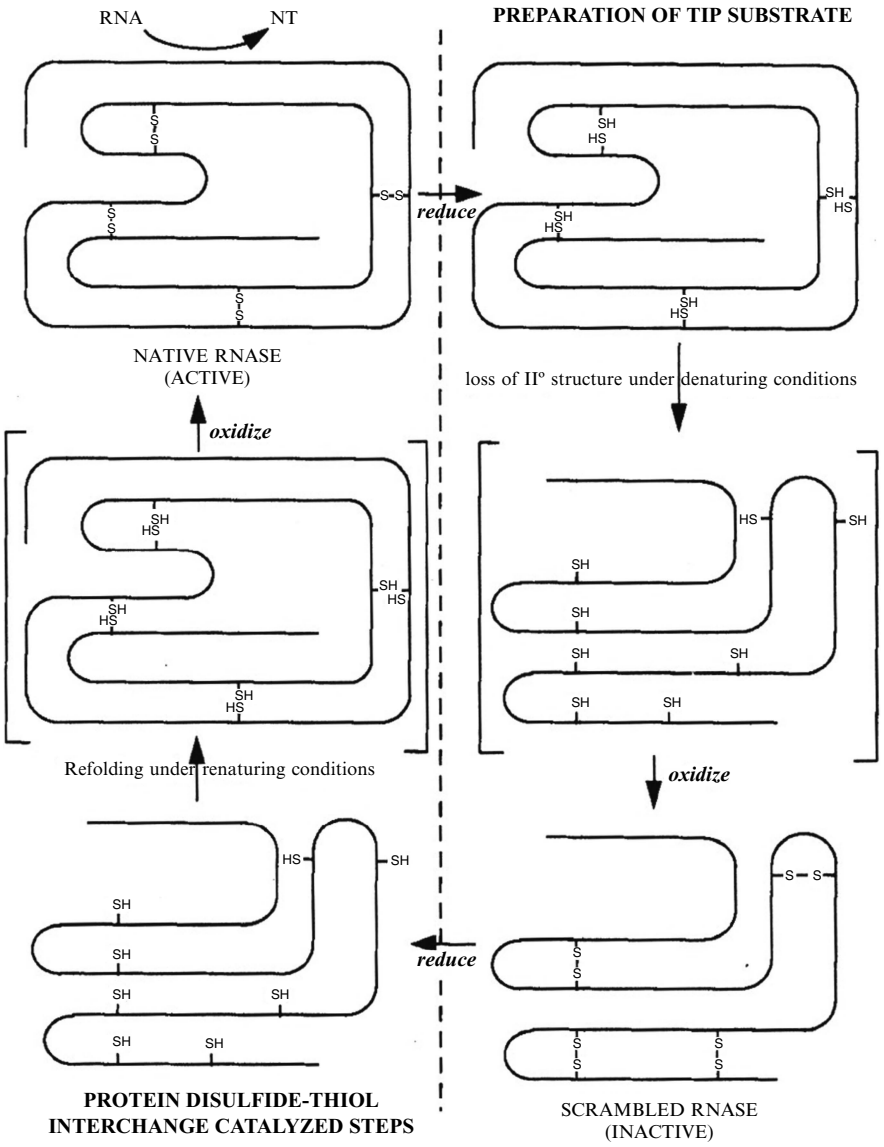

Fig. 2.17 Schematic representation of the procedure for preparation of scrambled and inactive RNase (*left*) and the restoration of activity through cleavage of disulfide bonds refolding under renaturating conditions and reformation of disulfide bonds as the protein disulfide-thiol interchange activity restores activity to the preparations

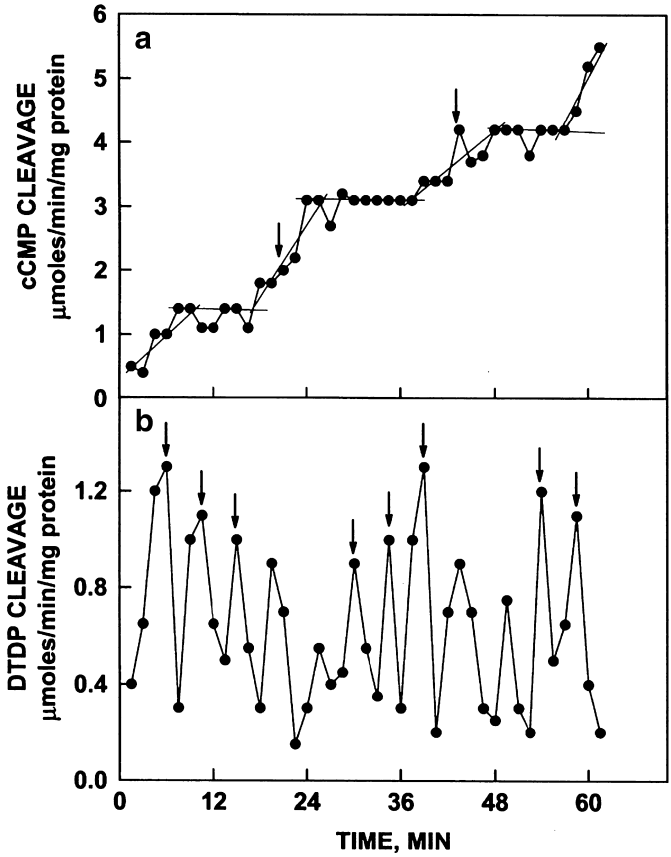

Fig. 2.18 Protein disulfide-thiol interchange activity of recombinant human ENOX1 measured from the activation of scrambled and inactive RNase to cleave cCMP measured spectrophotometrically (**a**) or from the cleavage of a DTDP substrate (**b**). Both activities exhibited an oscillatory activity. However, the activities were most strongly associated with the three maxima separated by 4.5 min rather than with the two maxima separated by 6 min dominated by oxidation of NADH. From Jiang et al. (2008) with permission from ACS publications

2.8 Estimates of Protein Disulfide-Thiol Interchange from Enzymatic Assay of Dipyridyl-Dithio Substrate Cleavage

The assay for the ability of 2,2′-dipyridyl-dithio substrates decompose to 2 mol of pyridinethione in buffered (50 mM Tris-Mes) aqueous solution at pH 7. The latter absorb strongly at 340 nM (Morré et al. 1999a). The assay was preincubated with 0.5 μmol 2,2′-DTDP or 6,6′-dithiodinicotinic acid (DTNA) in 5 μL of DMSO to react with endogenous reductants present with the plasma membranes. After 10 min, a further 3.5 μmol DTDP or DTNA were added in 35 μL DMSO to start the reaction. The final reaction volume was 2.5 mL.

The reaction was monitored from the increase in absorbance at 340 nm using a Hitachi Model U3210 spectrophotometer. The change in absorbance was recorded as a function of time by a chart recorder. Alternatively, absorbance changes were measured at 340 nm with reference at 430 nm using a SLM DW2000 spectrophotometer in the dual wavelength mode of operation. The specific activity was calculated using a millimolar absorption coefficient of 6.21/cm recognizing that 2 mol of product were generated for each mole of substrate cleaved (Fig. 2.17b).

The 2,2′-dipyridyl-dithio substrates were rapidly and completely hydrolyzed in the presence of reducing agents such as dithiothreitol and reduced glutathione (GSH). They were relatively more stable in the presence of the weak reducing agent cysteine and the weak oxidizing agent oxidized glutathione (GSSG). The substrates also spontaneously decompose such that it is necessary to subtract a blank rate with no enzyme present.

2.9 Measurement of *Trans*-Plasma Membrane Redox by Reduction of Cell-Impermeable Dyes

Artificial cell-impermeable dyes such as WST-1 (2-(4-iodophenyl)-3-(4-nitrophenyl)-5-(2,4-disulfophenyl)-2H-tetrazolium, monosodium salt) used in combination with mPMS (1-methoxy-5-methylphenazinium methyl sulfate) or coenzyme Q have been used to measure NADH oxidase driven plasma membrane electron transport (Tan and Berridge 2004; Figs. 2.19 and 2.20).

2.9.1 CoQ_1 Can Function as an Intermediate Electron Carrier in WST-1 Reduction

Cellular reduction of WST-1 involves an obligate intermediate electron carrier, namely, 1-methoxyPMS (Tan and Berridge 2004; Fig. 2.19). They also investigated whether CoQ_1, a homologue of CoQ_{10} with a short isoprenoid side chain and decreased lipophilicity could function as an alternative intermediate electron carrier. The results demonstrated that mPMS and CoQ_1 can directly access low potential electrons from the PMET system whereas WST-1 cannot. mPMS mediates electron transfer to WST-1 extracellularly, whereas CoQ_1 partitions in the plasma membrane.

2.9.2 Measurement of Plasma Membrane Electron Transport Based on WST-1 Reduction

Cells (2×10^4/0.1 mL for mPMS or 10^5/0.1 mL for CoQ_1) in HBSS, with or without mPMS or CoQ_1, were incubated in 96-well microtiter plates at 37 °C in a shaking

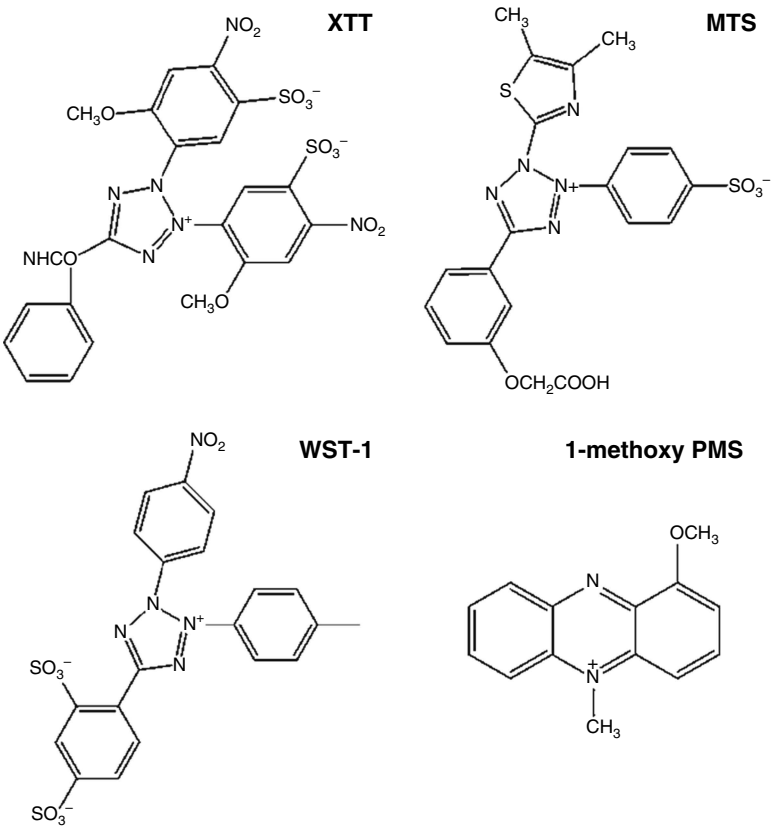

Fig. 2.19 Chemical structure of tetrazolium dye (XTT, MTF, and WST-1) and of the immediate electron acceptor 1-methoxy-5-methylphenazinium methyl sulfate (mPMS). Redrawn from Del Principe et al. (2011), Published with permission

BMG Fluostar microplate reader (Fig. 2.21). The reaction was initiated by adding 0.45 mM WST-1 followed by 25 μM mPMS or 50 μM CoQ_1 for 40 min. The absorbance was read in real time at 450 nm and the rate of WST-1 reduction as a measure of the activity of *trans*-plasma membrane electron transport is expressed as A_{450}/min (change in absorbance at 450 nm/min, multiplied by 1,000) (Tan and Berridge 2004).

For data of Fig. 2.21a, for example, when average rates were determined at 1.5-s intervals over 1 min at intervals of 1.5 min, oscillatory patterns characteristic of ENOX activities were observed (Fig. 2.22). Maxima corresponding to period lengths of 22 min (ENOX2), 24 min (ENOX1), or 26 min (arNOX) were evident from the analyses confirming the validity of using artificial cell-impermeable dyes in combination with mPMS to measure ENOX-driven plasma membrane electron transport.

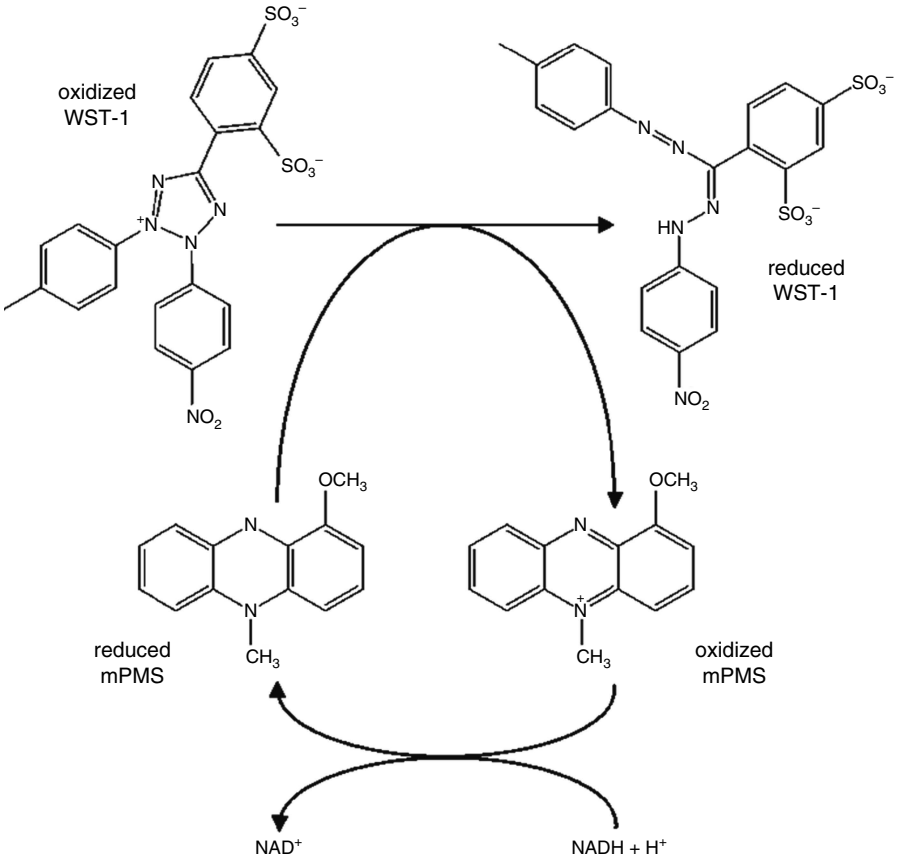

Fig. 2.20 Reduction of WST-1 (2-(4-iodophenyl)-3-(4-nitrophenyl)-5-(2,4-disulfophenyl)-2H-tetrazolium, monosodium salt) by the intermediate electron acceptor mPMS and formation of the reduced formazan. Redrawn from Del Principe et al. (2011), Published with permission

2.10 Summary

Spectroscopic strategies that substantiate periodic oscillations in low rates of NADH oxidation exhibited by ENOX proteins at the animal and plant cell surface are described. Both continuous display and discontinuous rate determinations exhibit the oscillations but continuous displays lack sufficient resolution to determine fine structural details. A procedure is documented where rates are determined by least squares analyses of traces recorded over 1 min at intervals of 1.5 min. These traces recapitulate the continuous displays but offer an opportunity to reliably estimate changes in reaction rates over short time intervals not afforded by the continuous traces. Turbidity is identified as the major contributor to losses in resolution. Even highly purified ENOX preparations tend to aggregate to form turbid suspensions.

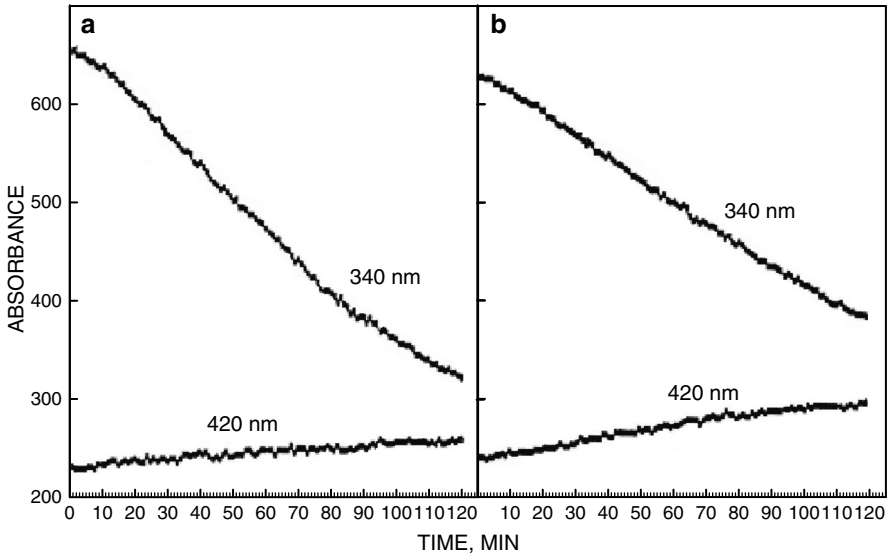

Fig. 2.21 Replicate measurements of NADH oxidase activity of intact 143B-osteocarcoma cells determined at 342 nm (with reference at 420 nm) based on the reduction of WST-1 in combination with mPMS (1-methoxy-5-methylphenazonium methyl-sulfate). Data courtesy of Dr. Michael Berridge, Malaghan Institute of Medical Research, Wellington, New Zealand, published with permission

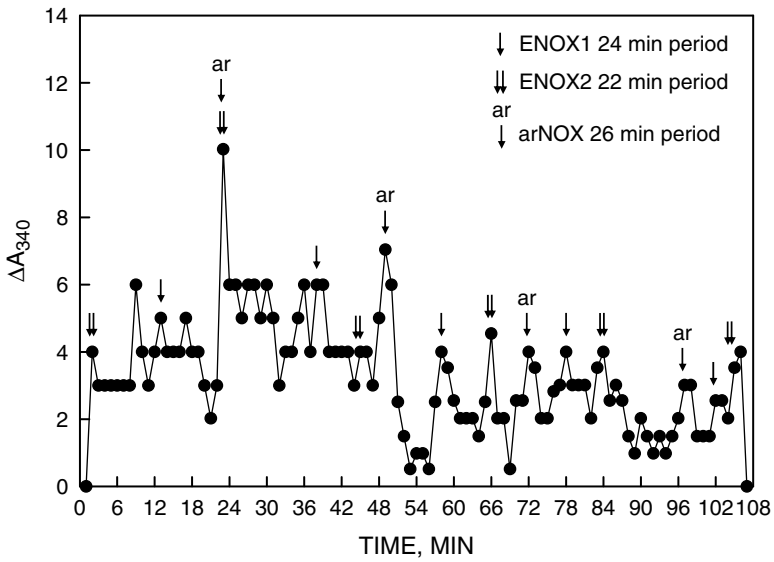

Fig. 2.22 Average rates from Fig. 2.21a determined at 1.5-s intervals averaged over 1 min and taken at intervals of 1.5 min reveal oscillatory patterns typical of established cultures of cancer cells expressing both ENOX1 and ENOX2 as well as the aging-related NADH oxidase (arNOX)

With turbid suspensions, double beam or dual wavelength instrumentation where the sample is placed immediately adjacent to the photomultiplier tube is required to reduce losses in resolution from turbidity. Also required are high levels of synchronous ENOX function. Blue or red (plants) light, small molecules (i.e., melatonin), electromagnetic fields, and autosynchrony alone or in combination may be used to synchronize the oscillations in asynchronous preparations. Special problems are posed by preparations containing more than one ENOX form that do not cross entrain, i.e., ENOX1 and ENOX2. Also described are assay methods based on hydroquinone (ubiquinol or phylloquinol) oxidation, and oxygen consumption for the oxidative activity and activation of scrambled RNase in the presence of cAMP substrate and from the cleavage of DTDP substrate measured spectrophotometrically for the protein disulfide-thiol interchange activity as well as the use of tetrazolium dyes.

http://www.springer.com/978-1-4614-3957-8

ECTO-NOX Proteins
Growth, Cancer, and Aging
Morré, D.J.; Morré, D.M.
2013, XVI, 508 p., Hardcover
ISBN: 978-1-4614-3957-8